Capillary Electrophoresis – Fourier Transform Ion Cyclotron Resonance Mass Spectrometry for the identification of Cationic Metabolites via a pH-Mediated Stacking–Transient Isotachophoretic method

Edward E.K. Baidoo[1,2*], *Peter I. Benke*[1,2*], *Christian Neusüß*[4], *Matthias Pelzing*[5], *Gary Kruppa*[6], *Julie A. Leary*[3], and *Jay D. Keasling*[1,2#]

[1]Department of Chemical Engineering, University of California, Berkeley, CA, U.S., [2]Physical Biosciences Division, Lawrence Berkeley National Laboratory, Berkeley, CA, U.S., [3]Genome Center, University of California, Davis, CA , U.S., [4]Aalen University, Aalen, Germany, [5]Bruker Biosciences, VIC, Australia, [6]Bruker Daltonics, CA, U.S.

#Corresponding author e-mail: keasling@berkeley.edu

Prof. Jay D. Keasling

Berkeley Center for Synthetic Biology,

717 Potter Street, Building 977,

University of California, Berkeley, CA, 94720-3224, USA.

Phone: (510) 495-2620

Fax: (510) 495-2630

*: These authors contributed equally in this study

February 19th, 2008.

ABSTRACT

Capillary electrophoresis-mass spectrometry (CE-MS) is still widely regarded as an emerging tool in the field of metabolomics and metabolite profiling. A major reason for this is a reported lack of sensitivity of CE-MS when compared to gas chromatography-mass spectrometry (GC-MS) and liquid chromatography-mass spectrometry (LC-MS). The problems caused by the lack of sensitivity are exacerbated when CE is coupled to fourier transform ion cyclotron resonance mass spectrometry (FT-ICR MS), due to the relatively low data acquisition rate of FT-ICR MS. Here, we demonstrate the use of an online CE sample preconcentration method, that uses a combination of pH-mediated stacking (PMS) and transient isotachophoresis (tITP), coupled with FT-ICR MS to improve the overall detection of cationic metabolites in the bacterium *Desulfovibrio vulgaris* Hildenborough (*D. vulgaris*). This method showed a significant increase in signal to noise when compared to CE normal sample stacking, while providing good separation efficiency, reproducibility, and linearity. Detection limits for selected amino acids were between 0.1 and 2 µM. Furthermore, FT-ICR MS detection consistently demonstrated good mass resolution and sub-ppm mass accuracy.

Key words: Metabolomics, Metabolite Profiling, pH-Mediated Stacking, Transient Isotachophoresis, CE-MS, Fourier Transform-Ion Cyclotron Resonance, *Desulfovibrio vulgaris* Hildenborough.

INTRODUCTION

The study of global metabolite profiles (metabolomics) can be represented by analytical spectra obtained from high throughput methods.[1] However, currently, there is not one method that can claim to separate, detect, and identify all metabolites, since no single technique is comprehensive, selective, and sensitive enough to measure them all. The primary reason for this is due to the structural diversity that exists within the metabolome.

Gas chromatography (GC) and mass spectrometry (GC-MS) remains a very widely used tool within the field of metabolomics.[2–9] However, since a large number of metabolites are non-volatile, time consuming derivatization steps are necessary to render them volatile; and thermally labile compounds, such as phosphorylated metabolites, can easily degrade when exposed to high temperatures within the gas chromatography (GC) oven. Furthermore, metabolites can have varying affinities for a derivatizing agent, which could lead to a bias in the results unless derivatized chemical standards are used to normalize for such a bias.

Direct infusion coupled with Fourier transform ion cyclotron resonance mass spectrometry (FT-ICR MS) allows for high resolution and accurate mass data sets of less than 1 ppm error [10–15] and can be utilized for non-targeted metabolome analysis of biological samples.[12–14] A major drawback of this technique is that it can be semi-quantitative as a result of ion suppression effects. However, when separation is conducted prior to detection, more quantifiable data can be obtained.

Direct infusion with nuclear magnetic resonance (NMR) is important for unequivocal determination of metabolite structure.[16–18] NMR also has lower sensitivity and a smaller dynamic range than MS and, like FT-ICR MS, is extremely expensive.

Liquid chromatography (LC) and mass spectrometry (LC-MS) can separate and detect a wide range of compounds and, along with GC-MS, LC-MS is also considered a very popular tool within the fields of metabolomics and metabolite profiling.[4,7,17,19–23] The major drawbacks of LC-MS can be the relatively low separation efficiency obtained when compared to GC-MS, the use of rather expensive columns

(which may be limited to particular classes of metabolites), and a large mobile phase consumption. However, the introduction of hydrophilic interaction liquid chromatography stationary phases [7,17] as well as new LC technologies, such as ultra performance LC,[20,22] which utilizes extremely high pressure to yield fast separations, have shown considerable improvement in separation efficiency and, in the case of nano LC,[23] reduced sample consumption.

Capillary electrophoresis (CE) and mass spectrometry (CE-MS) is an emerging tool in the field of metabolomics and metabolite profiling. In 2003, Soga and colleagues carried out a comprehensive and quantitative survey of anionic and cationic metabolites from *Bacillus subtilis* by CE-MS, showing that it was possible to use this technique for metabolome research.[24] Since that time, CE-MS has been used in various functional genomics studies.[17,25–30]

CE offers several potential advantages over GC and LC for the analysis of complex mixtures of metabolites, including high separation efficiencies, extremely small injection volumes (nL range), short analysis times, and low reagent costs. The main limitation of CE is its lack of sensitivity due to low injection volumes, especially when coupled to MS, as the sample can be further diluted by a sheath liquid that is delivered via a co-axial sheath flow interface. However, the combination of a reduced sheath flow rate (3μL/min and below) and the employment of online sample preconcentration procedures, such as pH-mediated stacking (PMS) and transient isotachophoresis (tITP), can achieve sensitivities similar to that of current LC-MS protocols.[31–33]

The successful online combination of CE with FT-ICR MS was previously demonstrated for the analysis of peptides and proteins,[34–37] the proteome of *Shewanella oneidensis*,[38] and complex pools of oligosaccarides.[39] However, the combination of CE and FT-ICR MS for the analysis of very low molecular weight compounds (i.e., metabolites < 250 Da) has not been demonstrated in the literature. The rapid separation of such compounds by CE can often yield very narrow peak widths and, as a result, lead to very few data points across a peak due to the relatively slow data acquisition rate of the FT-ICR MS, which can compromise sensitivity and limit the quantitative capability of this technique. Therefore,

a combination of PMS and tITP (PMS-tITP) has been utilized for online CE sample preconcentration with FT-ICR MS detection, in order to improve the overall detection of cationic metabolites in a bacterium.

The organism utilized for these studies is the anaerobic bacterium *Desulfovibrio vulgaris* Hildenborough (*D. vulgaris*). *D. vulgaris*, because of its metabolic versatility, its ability to remediate heavy metals and radionuclides, coupled with the ease with which it can be maintained in culture, is of particular interest to the U.S. Department of Energy (DOE). The sulfate reducing mechanisms within *D. vulgaris* allow this organism to reduce the oxidation states of various heavy metals and radionuclides, leading to the conversion of soluble to insoluble forms, thereby preventing their leaching into neighboring soils and ground water.[40–47] Thus, an understanding of regulatory mechanisms and cellular responses to different environmental factors affecting metal remediation, *in situ*, is of great importance.

EXPERIMENTAL SECTION

All chemical standards were obtained from Sigma-Aldrich, CA, USA. For CE-MS experiments, the above were prepared in one-tenth of the run electrolyte, which is 1.6 M formic acid in methanol and water (20:80, v/v). All chemicals used were of analytical and reagent grade, and all solvents used were of HPLC grade (Honeywell Burdick & Jackson, CA, USA). HPLC grade chloroform was obtained from Fisher Scientific (Pittsburg, PA, USA).

Desulfovibrio vulgaris Hildenborough (*D. vulgaris*) was obtained from ATCC and grown by the Terry Hazen laboratory, Lawrence Berkeley National Laboratory, CA, USA. *D. vulgaris* was cultured at 30°C in LS4D minimal media.[27] Growth was monitored by measuring the optical density at a wavelength of 600 nm (OD_{600}) via a Beckman DU 640 UV/Vis spectrophotometer (Beckman Coulter Inc., CA, USA). *D. vulgaris* was grown to an OD_{600} of 0.37.

Metabolite extraction. A *D. vulgaris* culture of 600 mL volume was centrifuged at 11,000 × g for 10 minutes at 4°C, after which the supernatant was decanted. To the remaining cell pellet, 20 mL of cold methanol (stored on dry ice) was added. A relatively small amount of the internal standard methionine

sulfone was spiked into the methanol prior to quenching. The centrifuge vial was then tapped vigorously in order to dislodge the cell pellet. After the cell pellet was fully mixed in methanol by vortexing, the methanol mixture was transferred to a 50-mL Falcon tube containing a cold chloroform/water (20 mL chloroform/7.7 mL water) mixture (stored on ice). After vortexing, the resulting mixture was centrifuged for 2 minutes at 6000 × g (at 4°C). The emerging two phases were further separated and left to settle on ice for approximately 2 minutes. The aqueous methanol/water layer (the top layer) was then transferred to a 50-mL Falcon tube. Approximately 30 mL of water was added to the aqueous layer and vortexed. The resulting mixture was frozen via liquid nitrogen and dried by lyophilization. The lyophilized sample was then reconstituted in 6 mL of water in preparation for solid phase extraction (SPE).

Solid Phase Extraction. SPE was carried out for the purpose of removing salts from the cell culture medium, which were in high concentration as a result of extensive preconcentration. A 1-g Oasis HLB SPE cartridge (Waters, MA, USA) was used throughout. For conditioning purposes, 10 mL of methanol followed by 10 mL of water were passed through the SPE cartridge sequentially. Then, 6 mL of sample was introduced into the cartridge followed by 10 mL of water. The sample was then eluted with 10 mL of methanol. To the eluted product, 20 mL of water was added and the resulting mixture was frozen via liquid nitrogen and dried by lyophilization. The dried product was then reconstituted with 100 μL of one-tenth of the run electrolyte in methanol and water (20:80, v/v). The resulting solution was centrifuged at 2000 × g (VWR Galaxy mini) at room temperature for 1 minute, after which the supernatant was collected and the precipitated protein pellet discarded.

Electrolyte and Sheath Liquid Preparation. Formic acid (Fisher Scientific, CA, USA) was dissolved in methanol and water (20:80, v/v). For the separation and detection of cations, 1.6 M formic acid (in methanol and water, 20:80, v/v) was used as the run electrolyte. The run electrolyte was filtered through a 0.2 μm syringe filter (Whatman Inc., NJ, USA) and degassed prior to analysis using a Branson

ultrasonic bath (Branson Ultrasonics, CT, USA). The sheath liquid was comprised of isopropanol and water (50:50 (v/v).

CE Conditions. CE separations were carried out in a 100 cm, 50 μm i.d. x 365 μm o.d. (total volume 1963 nl), untreated, fused silica capillary (PolyMicro Technologies, AZ, USA). The CE system (Agilent CE system, Agilent Technologies, CA, USA) utilizes programmable injection with pressure. Preconditioning of the capillary took place with 1 M NaOH (10 minutes at ~ 940 mbar in the flush mode), followed by the electrolyte (20 minutes at ~ 940 mbar in the flush mode). The capillary was conditioned prior to each run with 1.6 M formic acid in methanol and water (20:80, v/v) for 5 minutes at ~ 940 mbar in the flush mode. Ammonium hydroxide (12.5%) in methanol and water (20:80, v/v) was introduced to the capillary at 25 mbar for 5 seconds, after which the sample was introduced to the capillary at 50 mbar for 160 seconds for PMS-tITP. Sample introduction was followed by two sequential dips of the capillary inlet in two separate vials containing water to prevent carry over into the next sample. Formic acid at a concentration of 4 M in methanol and water (20:80, v/v) was then introduced to the capillary at 50 mbar of pressure for 12 seconds. Separations in the positive mode of CE were achieved by using an applied voltage of +30 kV. The electrolyte was replenished after every three run cycles to account for electrolyte depletion. For normal sample stacking experiments, the same conditioning procedures were applied. Here, the sample was introduced to the fused silica capillary at 50 mbar for 3 seconds. This was followed by the introduction of a 1.6 M formic acid, in methanol and water (20:80, v/v), plug at 50 mbar for 12 seconds. When a large volume of sample was introduced to the fused silica capillary, the same injection parameters, as the PMS-tITP method, were used.

In these experiments, CE/ESI/MS coupling was achieved using an orthogonal coaxial sheath-flow interface. The Agilent CE system was interfaced to the corresponding MS via a G1603A Agilent CE-MS adapter kit and a G1607A Agilent CE-ESI-MS sprayer kit (Agilent Technologies, CA, USA). Grounding of the CE-ESI-MS sprayer ensured that a full +/- 30 kV potential difference was applied across the length of the capillary for more efficient separation.

CE ESI Single Quadrupole MS Conditions. An Agilent LC/MSD SL mass spectrometer (Agilent Technologies, CA, USA) was used for tITP-PMS method optimization and repeatability experiments. An Agilent 1100 series isocratic pump (Agilent Technologies, CA, USA) was used to deliver the sheath liquid. Agilent CE system and LC/MSD SL were controlled by the Chemstation (Agilent Technologies, CA, USA) software package. Contact between both instrument set-ups was established by a LAN card in order to trigger the MS into operation upon the initiation of a run cycle from Chemstation. ESI-MS was conducted in the positive ion mode and a capillary voltage of + 4000 V was utilized. MS experiments were carried out in the selected ion monitoring mode for the detection of $[M + H]^+$ ions. The instrument was tuned for a range of 50 – 2000 m/z.

The LC/MSD SL was calibrated externally by the Agilent ES tune mix (Agilent Technologies, CA, USA). Data acquisition and processing was carried out by the Chemstation software package.

Nitrogen gas was used as both the nebulizing and drying gases to facilitate the production of gas-phase ions. The drying and nebulizing gases were set to 3 L/min and 4 psi respectively and a drying gas temperature of 180 °C was used throughout. An electrical contact at the outlet end was provided by the sheath liquid at a flow rate of 3 µL/min.

CE ESI TOF MS Conditions. A Bruker MicrOTOF time of flight mass spectrometer (Bruker Daltonics, CA, USA) was used for repeatability experiments. A Harvard syringe pump (Harvard Apparatus, MA, USA) was used to deliver the sheath liquid. Both the Agilent CE system and the Bruker MicrOTOF were controlled by Chemstation (Agilent Technologies, CA, USA) and Compass (Bruker Daltonics, CA, USA) software packages respectively. A contact closure between both instrument set-ups was established in order to trigger the MS into operation upon the initiation of a run cycle from Chemstation. ESI-MS was conducted in the positive ion mode and a capillary voltage of + 4500 V was utilized. MS experiments were carried out in full scan mode, at two times the rolling average and 25,000 summations, for the detection of $[M + H]^+$ ions. The instrument was tuned for a range of 50 – 350 m/z.

The MicrOTOF was calibrated, pseudo-internally, by a mixture of amino acids (each at 10 µM concentration), which were dissolved in a solvent mixture of isopropanol and water (50:50, v/v) and

delivered by a 20 µL injection loop, via a Cole Parmer syringe pump (Cole Parmer, IL, USA), prior to each run. Data acquisition and processing was carried out by the Compass software package.

Nitrogen gas was used as both the nebulizing and drying gases to facilitate the production of gas-phase ions. The drying and nebulizing gases were set to 3 L/min and 0.3 bar respectively and a drying gas temperature of 180 °C was used throughout. An electrical contact at the outlet end was provided by the sheath liquid at a flow rate of 3 µL/min.

CE ESI FT-ICR MS Conditions. A Bruker Apex Qe Fourier transform ion cyclotron resonance mass spectrometer (FT-ICR MS) was used for CE-FT-ICR MS experiments (Bruker Daltonics, CA, USA). Grounding of the CE-ESI-MS sprayer ensured that a full + 30 kV potential difference was applied across the length of the capillary for more efficient separation. The Agilent CE system and the Bruker Apex Qe FT-ICR MS were controlled by Chemstation (Agilent Technologies, CA, USA) and Apex control (Bruker Daltonics, CA, USA) software packages, respectively. A contact closure between the instruments was established in order to trigger the FT-ICR MS into operation upon the initiation of a run cycle from Chemstation. Nitrogen gas was used as both the nebulizing and drying gases to facilitate the production of gas-phase ions. The drying and nebulizing gases were set to 3 L/min and 0.3 bar, respectively, and a drying gas temperature of 180°C was used throughout. An electrical contact at the outlet end was provided by the sheath liquid at a flow rate of 3 µL/min. The Apex Qe FT-ICR MS was equipped with a Bruker-Magnex actively shielded superconducting magnet at 9.4 Tesla. ESI FT-ICR MS was conducted in the positive ion mode via an Apollo I ESI source. A capillary voltage of –4461 V was utilized on the inlet of the glass capillary, –4000 V on the outlet of the glass capillary, and –2000 V was applied to the cylinder shield. The capillary exit voltage was set to 75 V. Ions were accumulated in an external hexapole in the source region of the FT-ICR MS for 1.0 second before transfer to the FT-ICR MS analyzer cell. Data was acquired over the mass range from m/z 65 to 1000, resulting in a sweep width of 2.0 MHz, with a transient data set size of 131,072 points. This resulted in a transient length of 32.8 msec. No averaging of transients was employed, the single transient was transformed to a data set

size of 131,072 points and calibrated in the Bruker Daltonics DataAnalysis 3.4 software package (Bruker Daltonics, CA, USA). The ion accumulation time of 1.0 second, when added to the transient acquisition time of 32.8 msec and other fixed delays and data transfer time, resulted in a time between recorded mass spectra of 1.3 sec. The conditions described were found to give the optimum FT-ICR MS detection of compounds within the ranges of 90 to 250 m/z and 76 to 250 m/z for the Apollo I and II sources respectively. The Apollo II source was used for the repeatability study. A Cole Parmer syringe pump (Cole Parmer, IL, USA) was used for sheath liquid delivery. The Apex Qe FT-ICR MS was calibrated externally for the positive ion mode using a standard mixture of amino acids (10 μM), which were dissolved in a solvent mixture of isopropanol and water (50:50, v/v). A subsequent internal calibration of the m/z axis, with selected amino acids from the sample mixture, was employed via DataAnalysis 3.4.

RESULTS AND DISCUSSION

Narrow peak widths are a common feature of CE separations, especially when no supplementary pressure is applied. Since a typical CE peak can have a width of about 10 seconds, it was decided that the total scan time of the FT-ICR MS be reduced to 1.3 seconds, which meant that there was approximately 7.7 points across the CE peak. Generally, the more data points acquired across a CE or chromatographic peak, the higher the quality of chromatographic data and hence an increase in the quantitative information obtained. The aforementioned total ion scan time was found to be sufficient to perform our MS experiments, but there was a noticeable reduction in the resolving power of the instrument. For a fixed FT-ICR transient acquisition time, the resolution in FT-ICR MS is known to be inversely proportional to the mass.[48,49] In this case the transient acquisition time of 32.8 msec resulted in a resolution of 15,000 at m/z 250 and 30,000 at m/z 125. For the purpose of our experiments the combination of CE separation and FT-ICR MS was more than adequate, in terms of resolution and mass accuracy, for the identification of metabolites, including structural isomers.

Two, online, sample preconcentration procedures were utilized in order improve the overall sensitivity of FT-ICR MS detection of analytes separated by CE. The first methodology was normal sample stacking. This approach has been used in various studies in metabolomics and metabolite profiling.[24,25,27–30] Here, the sample was dissolved in one-tenth of the run electrolyte (Figure 1), which results in the sample zone having a lower ionic strength and, consequently, a lower conductivity than the run electrolyte. Thus, when a voltage is applied, a higher electric field strength is generated within the sample plug than in the run buffer due to a higher resistivity. Since electrophoretic velocity is proportional to electric field strength, the solute ions will migrate rapidly through the dilute sample plug until they reach the concentration boundary between the sample plug and the run buffer. The solute ions then encounter a reduced electric field strength at this boundary and therefore slow down, forming a narrow, stacked zone. They will then proceed through the capillary, under the influence of their electrophoretic mobilities, as stacked zones that are narrower than the sample plug (Figure 1). At 1.6 M

formic acid, the run electrolyte has a pH of approximately 1.8, which should bring about the neutralization of the inner surface of the fused silica capillary.[24] At this pH, the majority of the silanoate groups on the inner surface of the fused silica will be protonated to silanol. Thus, the electroosmotic flow is close to zero and has very little influence on the stacking process and the electrophoretic separation.

The CE-FT-ICR MS analysis of a mixture of 17 amino acid standards (at 50 µM concentrations for all standards except cystine, which was at 25 µM concentration) revealed that some of the low abundant ions such as lysine, aspartate, serine, alanine and cystine were not detected by normal sample stacking (but were detected by the PMS-tITP method). A key reason for the lack of sensitivity was the relatively low amount of sample injected onto the column (i.e., a sample volume of 2.5 nL). Thus, a large volume sample preconcentration strategy was required.

In 2005, Gillogly and Lunte described a PMS procedure that utilized electrokinetic injection of a strong acid plug to titrate against acetate ions in the sample zone.[32] This created a region of low conductivity neutralized acetic acid across which cationic analytes were stacked.[32] Electrokinetic injection, however, may lead to a bias towards higher mobility analytes. In 2002, Neusüß *et al.* described a PMS procedure that utilized formic acid to titrate against NH_3 in the sample zone for peptide analysis.[31] A slightly modified version of the latter approach, which utilizes PMS-tITP online preconcentration, was used for all CE experiments in this study, primarily because there is no bias towards higher mobility analytes as a result of hydrodynamic sample introduction (Figure 2).

A possible explanation for the concentration of analytes by our PMS-tITP procedure is that upon the application of a voltage, H^+ from the 4 M formic acid plug enters the sample zone and, together with H^+ already present in the sample zone, are titrated against OH^- ions from the NH_4OH plug, which also enter the sample zone in the direction of the anode, creating a zone of high resistivity.[32] During the process of titration, analytes are stacked into narrow bands at the boundary of the titrated region and the background electrolyte (BGE). In the case of zwitterionic species, such as amino acids, ions are

negatively charged when entering the basic zone and positively charged when entering the acidic zone. Thus, the OH^- boundary forces the zwitterionic amino acids towards the anode and, from the opposite side, the H^+ boundary forces them towards the cathode. As a result, analytes form sharp, narrow stacked bands, after which they will migrate towards the cathode by way of their electrophoretic mobilities. This is the PMS portion of the stacking procedure (Figure 2). At the same time, the tITP process should also be taking place. In tITP, the sample plug is placed between the leading electrolyte (leading ion NH_4^+) and terminating electrolyte (terminating ion H^+)[50] in the capillary, and a voltage is applied (Figure 3). Leading electrolyte ions have greater mobilities than solute ions present in the sample, whilst terminating electrolyte ions have the lowest mobilities.[51–53] Formic acid is used as a terminating electrolyte because migration of the terminating ion, H^+, is hindered by the buffering mechanism of the counter ion ($HCOO^-$).[54] At the point of focusing, cations in the sample arrange themselves in order of mobility, with those of the highest mobility next to the leading electrolyte, whilst those of the lowest mobility are next to the terminating electrolyte.[55] After solutes distribute themselves in the capillary, an equilibrium is reached, whereby all electrolyte and solute cations migrate at the same velocity, the velocity of the leading cations,[52] for a transient period of time. Analytes can then migrate towards the cathode as a result of their electrophoretic mobilities.

In order to optimize the PMS-tITP method, the relationships of peak height, peak area and peak-to-peak resolution to the percentage of ammonium hydroxide (varied from 0 to 20 %) were tested in triplicate measurements. From the results obtained, the peak height appeared to reach its maximum value between 5 and 20 % of ammonium hydroxide (Supporting Information Figure 1), the peak area was relatively unchanged, and the peak-to-peak resolution (R), [52] via methionine sulfone, was found to be highest between the range of 10 and 15 % of ammonium hydroxide. Since 10 to 15 % of ammonium hydroxide appeared to be optimal for peak height and resolution, 12.5 % of ammonium hydroxide was chosen for all PMS-tITP experiments.

To demonstrate the pre-concentrating power of PMS-tITP, the method was compared to normal sample stacking under small (at 2.5 nL) and large (134 nL) sample injection volumes. The internal standard, methionine sulfone, was used to make these comparisons. Sample injection volumes were calculated via the Beckman CE Expert software package for generic CE systems, in which parameters such as temperature (20°C), injection pressure (50 mbar), injection time (in seconds), viscosity relative to water (taken as 0.91 cP), and capillary dimensions were taken into account. Results show that when a large volume of sample is introduced into the fused silica capillary via normal sample stacking, significant peak broadening is observed (Figure 4) and indicates that very little stacking took place. This observation is made all the more obvious when the large volume of sample injected is compared to a small volume of sample injected (at 2.5 nL) under the same normal sample stacking conditions. In this case, the small volume of sample injected, via normal sample stacking, produces a methionine sulfone peak that is clearly more resolved (Figure 4). An experiment showing the maximal volume of sample introduced, via normal sample stacking, that is required to yield a resolved methionine sulfone peak was not conducted. When PMS-tITP was conducted with a large volume (134 nL) of sample injected into the fused silica capillary, a highly resolved methionine sulfone peak was observed. Furthermore, this peak was on the order of 8 and 20 times the signal intensity of the large and small volume normal sample stacking procedures, respectively.

The comparison of PMS-tITP and normal sample stacking was expanded further to include selected amino acids (Tables 1). A comparison of peak areas of the amino acid standards obtained from normal sample (at 2.5 nL sample injection volume) and pH-mediated (at 134 nL sample injection volume) stacking procedures indicates that all amino acids, with the exception of isoleucine, showed >20-fold increase in their peak areas for PMS-tITP when compared to normal sample stacking (Table 1). A comparison of peak heights of the amino acid standards obtained from normal sample stacking and PMS-tITP procedures indicates that all amino acids, with the exception of arginine and phenylalanine, showed >15-fold increase in peak height for PMS-tITP when compared to normal sample stacking. Thus, the results clearly show the pre-concentrating power of PMS-tITP.

After demonstrating the pre-concentrating power of PMS-tITP, it is important to demonstrate the separating power of the technique. The resolution obtained for amino acids from normal sample stacking (with large and small injection volumes) and PMS-tITP was compared (Table 2). Methionine sulfone was used as the reference peak to calculate resolution for the selected amino acids. For normal sample stacking, sample injection volumes of 2.5 and 134 nL were used for amino acid standards at concentrations of 50 µM. For PMS-tITP, a sample injection volume of 134 nL was used for *D. vulgaris* lysate, and amino acid standards at concentrations of 3.12 and 50 µM were also used. In all cases, resolution was highest for normal sample stacking with a 2.5-nL sample injection volume. Not surprisingly, normal sample stacking with a 134-nL sample injection volume showed the lowest resolution for all amino acids, with respect to methionine sulfone. For PMS-tITP, the resolution, in all cases, was higher than for normal sample stacking with a 134-nL sample injection volume, but was lower than for normal sample stacking with a 2.5-nL sample injection volume. Interestingly, the resolution obtained for selected amino acids from the *D. vulgaris* lysate and amino acid standard mixtures at 3.12 and 50 µM concentrations were found to be reasonably consistent.

When looking at separation, one has to also consider the number of theoretical plates, *N*, which is a measure of how powerful the separation is. The number of theoretical plates can be calculated by

$$N = 16(t/w)^2$$

where t is the migration time and w is the peak width.[52]

For normal sample stacking, sample injection volumes of 2.5 and 134 nL were used for amino acid standards at concentrations of 50 µM. For PMS-tITP, a sample injection volume of 134 nL was used for *D. vulgaris* lysate, and amino acids standards at concentrations of 3.12 and 50 µM were also used. Typically, all amino acids showed numbers of theoretical plates >100,000 for normal sample stacking with a 2.5 nL injection volume (Table 3). But normal sample stacking with an injection volume of 134 nL showed numbers of theoretical plates <10,000 for selected amino acids. For PMS-tITP, there was a significant increase in the number of theoretical plates observed when the concentration was reduced from 50 to 3.12 µM. Interestingly, the number of theoretical plates for isoleucine and leucine were

similar for both normal sample stacking (at 2.5 nL injection volume) and PMS-tITP. There was a further increase in the number of theoretical plates observed for amino acids from the *D. vulgaris* sample. This was probably due to the presence of amino acids at lower concentrations. But it was surprising to see some amino acids with theoretical plate numbers >1,000,000. It is likely that the limited ability of the FT-ICR-MS to collect many data points across a peak (i.e., >10 data points at a minimum resolving power of 15,000) for the low abundant ions was responsible for such high theoretical plate numbers. In any case, it appears that the pre-concentrating power of PMS-tITP is ideal for the measurement of low abundance, cationic species, since the relatively high theoretical plate numbers achieved can compensate for a slight reduction in electrophoretic peak-to-peak resolution (as compared to the resolution exhibited by normal sample stacking). PMS-tITP was also effective in the separation of structural isomers such as isoleucine and leucine. Furthermore, when introducing a large volume of sample (134 nL) into the capillary, a significantly higher peak capacity was achieved for the PMS-tITP method than for normal sample stacking, even though the elution time window was shorter for the former (Supporting Information Table 1). Thus PMS-tITP, when coupled to FT-ICR MS, appears to be more than adequate for the metabolite analysis.

In order to fully validate the method, linearity and precision were also tested. Good linearity was observed for selected amino acids (Table 4). Furthermore, the limits of detection for selected amino acids, with the exception of methionine and tyrosine, were sub-μM. These results indicate that the PMS-tITP, CE-FT-ICR MS, method can be used for quantitative measurements of metabolites.

CE is generally more susceptible to changes in temperature, pH, buffer concentration and ionic strength, all of which may affect the reproducibility of CE measurements. It was therefore imperative that the technique demonstrate good reproducibility. Thus, a careful study of repetitive analyses was required to validate the method. To fully evaluate the method, three different types of mass analyzer (quadrupole, TOF, and FT-ICR) were used in three different locations and on three different days. The results presented in Supporting Information Table 2 showed very good % relative standard deviation (RSD) for migration times, as indicated by the low % RSDs obtained for fifteen repetitive

measurements. Relative migration times (the ratio of the compound migration time to the internal standard migration time) produced even lower % RSD values over the same number of measurements in nearly all cases. Nebulizing and drying gas flow rates, however, were not accurately controlled by the Apollo sources of the Bruker FT-ICR MS. As a result, a high nebulizer pressure was observed at the tip of the CE sprayer, which could affect CE separation by shortening migration times. It is possible the high nebulizer pressure could create a region of low pressure at the tip of the fused silica capillary, thereby causing a sucking effect at this point, which could generate a faster flow through the capillary, and hence a reduction in separation efficiency due to the formation of a laminar flow profile. Moreover, a less accurate nebulizing gas flow rate gauge could also explain the higher migration time and peak area % RSD observed with FT-ICR MS, when compared to Quad MS and TOF MS. The average peak area % RSDs for Quad MS, TOF MS and FT-ICR MS were 5.5, 5.4 and 6.8 respectively. These values were higher than migration time errors but, with the good linearity observed from CE-FT-ICR MS measurements (Supporting Information Figure 2, Table 4), should be adequate for quantitative analysis. This method can therefore be very useful for comprehensive analyses of cations from biological extracts.

Application of CE-FT-ICR MS to *D. vulgaris* metabolites. The applicability of the CE-FT-ICR MS method to metabolic intermediates was demonstrated on *D. vulgaris* lysate (Figure 5). Identification of metabolites can be made possible through accurate mass measurements and empirical formula generation. However, when considering structural isomers (e.g., isoleucine and leucine), accurate mass measurements alone do not provide conclusive identification, as several compounds can have the same empirical formula and hence the same molecular mass. In such cases, the elution order from CE separation is required for identification with a high degree of confidence. This can be obtained by comparing the elution time of the compound of interest with a chemical standard. Such an approach can be referred to as targeted analysis. The metabolites listed in (Table 5) were identified using this methodology. Since relative migration times were found to yield lower % RSDs than those of migration times alone (Supporting Information Table 2), relative migration times were therefore utilized in

conjunction with accurate mass measurements for the identification of metabolites. From the 27 metabolites identified, 74% were of sub-ppm mass accuracy, and only two gave mass errors at 3 ppm. This targeted approach has revealed the presence of cationic metabolites from classes of compound such as amino acids, polyamines, purines and pyrimidines.

The selection of metabolites that were observed can be utilized to gain possible insights into specific aspects of *D. vulgaris* metabolism (Table 5). For example, spermine and spermidine can play significant roles in many biological processes, but their molecular functions, in vivo, are still not clearly understood. Glutamate and glutamine play important roles in the assimilation of NH_4^+ into amino acids. Glutamate is also reported to play a key role as an osmo-protectant against bacterial salt stress and adaptation.[27] Methionine production can also be correlated to an active sulfur metabolism and is therefore a key indicator of the sulfate reducing capability of *D. vulgaris*. However, not all genes for methionine biosynthesis in *D. vulgaris* are annotated, so a targeted approach could yield important information with regards to this biosynthetic pathway as well as the sulfur metabolism/reduction pathway.

However, the 27 metabolites targeted in *D. vulgaris* lysate (Table 5) represent only a small fraction of the total metabolite pool. Thus, obtaining chemical standards for the construction of an extensive database for the remaining metabolites of the major *D. vulgaris* pathways should ensure the characterization of metabolism in this organism as fully as possible via the identification of unknowns.

CONCLUSIONS

A robust, PMS-tITP CE-FT-ICR MS method was presented for the analysis of cationic species. This method showed a significant increase in signal to noise when compared to normal sample stacking, while providing good separation efficiency, reproducibility, and linearity. FT-ICR MS detection demonstrated high mass accuracy and high m/z resolution. Thus, CE-FT-ICR MS should be considered a technique of high resolution, with a potential to provide highly quantitative data. The effectiveness of the method was demonstrated by the successful analysis of metabolic intermediates from several metabolic pathways in *D. vulgaris.* The results indicate that the method can be a useful tool for the identification of cationic metabolites and has the potential to be utilized for metabolomics research in all organisms. Moreover, this PMS-tITP method was successfully coupled to FT-ICR MS, TOF and quadrupole mass spectrometers and should therefore be applicable to other MS technologies.

ACKNOWLEDGEMENTS

This work is part of the Virtual Institute for Microbial Stress and Survival (http://vimss.lbl.gov) and supported by the U.S. Department of Energy, Genomic:GTL Program through contract DE-AC02-05CH11231 between the Lawrence Berkeley National Laboratory (LBNL) and the U.S. Department of Energy. We thank the Hazen laboratory (Terry C. Hazen, LBNL) for providing biomass samples.

References

(1) Schmidt, C., *J. Nation. Canc. Inst.* **2004**, 96, 732–734.

(2) Bino, R. J.; Hall, R. D.; Fiehn, O.; Kopka, J.; Saito, K.; Draper, J.; Nikolau, B. J.; Mendes, P.; Roessner-Tunali, U.; Beale, M. H.; Trethewey, R. N.; Lange, B. M.; Wurtele, E. S.; Sumner, L. W., *Trends Plant Sci.*, **2004**, 9, 418–425.

(3) Fiehn, O.; Kopka, J.; Dormann, P.; Altmann, T.; Trethewey, R. N.; Willmitzer, L., *Nat. Biotechnol.*, **2000**, 18, 1157–1161.

(4) Nikiforova, V. J.; Kopka, J.; Tolstikov, V.; Fiehn, O.; Hopkins, L.; Hawkesford, M. J.; Hesse, H.; Hoefgen, R., *Plant Physiol.*, **2005**, 138, 304–318.

(5) Kind, T.; Fiehn, O., *BMC Bioinformatics*, **2006**, 7, Art no. 234.

(6) Kind, T.; Fiehn, O., *BMC Bioinformatics*, **2007**, 8, Art. no.105.

(7) Kind, T.; Tolstikov, V.; **Fiehn, O**.; Weiss, R. H., Analytical Biochemistry, **2007**, 363, 185–195.

(8) Lommen, A.; van der Weg, G.; van Engelen, M. C.; Bor, G.; Hoogenboom, L. A. P.; Nielen, M. W. F., *Anal. Chim. Acta*, **2007**, 584, 43–49.

(9) Mas, S.; Villas-Boas, S. G.; Hansen, M. E.; Akesson, M.; Nielen, J., *Biotech. & Bioeng.*, **2007**, 96, 1014–1022 .

(10) Marshall, A. G.; Hendrickson, C. L.; Jackson, G. S., *Mass Spec. Rev.*, **1998**, 17, 1–35.

(11) Pingitore, F.; Tang, Y.; Kruppa, G.; Keasling, J., *Anal. Chem.*, **2007**, 79, 2483–2490.

(12) Aharoni, A.; Ric De Vos, C. H.; Verhoeven, H. A.; Maliepaard, C. A.; Kruppa, G.; Bino, R.; Goodenowe, D. B., *A J. Interg. Biol.*, **2002**, 6, 217–234.

(13) Brown, S. C.; Kruppa, G.; Dasseux, J.-L., *Mass Spec. Rev.*, **2005**, 24, 223–231.

(14) Oikawa, A.; Nakamura, Y.; Ogura, T.; Kimura, A.; Suzuki, H.; Sakurai, N., Shinbo, Y.; Shibata, D.; Kanaya, S.; Ohta D, *Plant Physiol.*, **2006**, 142, 398–413.

(15) Kai, K.; Tatsumi, M.; Shibata, D.; Kanaye, S.; Ohta, D., Plant & Cell Physiol., **2007**, 48, S68-S68.

(16) Lindon, J. C.; Holmes, E.; Nicholson, J. K., *Anal. Chem.*, **2003,** , 385 A–391 A.

(17) McNally, D. J., Hui, J. P. M.; Aubry A. J.; Mui, K. K. K.; Guerry, P.; Brisson, J.-R.; Logan, S. M., Soo., E. C., *J. Bio. Chem.*, **2006**, 281, 18489–18498.

(18) Cloarec, O.; Campbell, A.; Tseng, L. H.; Braumann, U.; Spraul, M.; Scarfe, G.; Weaver, R.; Nicholson, J. K., *Anal. Chem.*, **2007**, 79, 3304–3311.

(19) Buchholz, A.; Hurlebaus, J.; Wandrey, C.; Takors, R., *Biomol. Eng.*, **2002**, 19, 5–15.

(20) Wilson, I. D.; Nicholson, J. K.; Castro-Perez, J.; Granger, J. H.; Johnson, K. A.; Smith, B. W.; Plumb, R. S., *J. Prot. Res.*, **2005**, 4, 591–598.

(21) Wu, L.; Mashego, M. R.; van Dam, J. C.; Proell, A. M.; Vinke, J. L.; Ras, C.; van Winden, W. A.; van Gulik, W. M.; Heijnen, J. J., *Anal. Chem.*, **2005**, 336, 164–171.

(22) Nordstrom, A.; O'Maille, G.; Qin, C.; Siuzdak, G., *Anal. Chem.*, **2006**, 78, 3289–3295.

(23) Want, E. J.; O'Maille, G.; Smith, C. A.; Brandon, T. R.; Uritboonthai, W.; Qin, C.; Trauger, S. A.; Siuzdak, G., *Anal. Chem.*, **2006**, 78, 743–752.

(24) Soga, T.; Ohashi, Y.; Ueno, Y.; Naraoka, H.; Tomita, M.; Nishioka, T. *J. Prot. Res.*, **2003**, 2, 488–494.

(25) Sato, S.; Soga, T.; Nishioka, T.; Tomita, M., *The Plant J.*, **2004**, 40, 151–163.

(26) Soo, E.C.; Aubry, A. J.; Logan, S. M.; Guerry, P.; Kelly, J. F.; Young, N. M.; Thibault, P. *Anal. Chem.*, **2004**, 76, 619–626.

(27) Mukhopadhyay, A.; He, Z.; Alm, E. J.; Arkin, A. P.; Baidoo, E. E.; Borglin, S. C.; Chen, W.; Hazen, T. C.; He, Q.; Holman, H.-Y.; Huang, K.; Huang, R.; Joyner, D. C.; Katz, N.; Keller, M.; Oeller, P.; Redding, A.; Sun, J.; Wall, J.; Wei, J., Yang, Z.; Yen, H.-C.; Zhou, J.; Keasling, J. D., *J. Bacteriol.*, **2006**, 188, 4068–4078.

(28) Saito, N.; Robert, M.; Kitamura, S.;Baran, R.; Soga, T.; Mori, H.; Nishioka, T.; Tomita, M., *J.*

Proteome Res., **2006**, 5, 1979–1987.

(29) Soga,T.; Baran, R.; Suematsu, M.; Ueno, Y.; Ikeda, S.; Sakurakawa, T.; Kakazu, Y.; Ishikawa, T.; Robert, M.; Nishioka, T.; Tomita, M., *J*. *Biol*. *Chem*., **2006**, 281, 16768–16776.

(30) Tanaka, Y.; Higashi, T.; Rakwal, R.; Wakida, S.-I.; Iwahashi, H., *J*. *Pharmaceut*. *Biomed*. *Anal*., **2007**, In press.

(31) Neusüß, C.; Pelzing, M., Macht, M., *Electrophoresis*, **2002**, 23, 3149–3159.

(32) Gillogly, J. A.; Lunte, C. E.; *Electrophoresis*., **2005**, 26, 633–639.

(33) Lee, R.; Ptolemy, A. S.; Niewczas, L.; Britz-Mckibbin, P., *Anal*. *Chem*., **2007**, 79, 403–415.

(34) Hofstadler, S. A.; Wahl, J. H.; Bruce, J. E.; Smith, R. D., *J*. *Am*. *Chem*. *Soc*., **1993**, 115, 6983–6984.

(35) Hofstadler, S. A.; Swanek, F. D.; Gale, D. C.; Ewing A. G.; Smith, R. D., *Anal*. *Chem*., **1995**, 67, 1477–1480.

(36) Hofstadler, S. A.; Severs, J. C.; Smith, R. D.; Frank, D. Swanek, F. D.; Ewing, A. G., *J*. *High Resol*. *Chromatogr*., **1996**, 19, 617–621.

(37) Jensen, P. K.; Paša-Tolić; Peden, K. K.; Martinović, S.; Lipton, M. S.; Anderson, G. A.; Tolić, N.; Wong, K.-K.; Smith, R. D., *Electrophoresis*. **2000**, 21, 1372–1380.

(38) Mohan, D.; Paša-Tolić, L.; Masselon, C. D.; Tolić, N.; Bogdanov, B.; Hixson, K. K.; Smith, R. D.; Lee, C. S., *Anal*. *Chem*. **2003,** 75, 4432–4440.

(39) Que, A. H.; Mechref, Y.; Huang, Y.; Taraszka, J. A.; Clemmer, D. E.; Novotny, M. V., *Anal*. *Chem*., **2003,** 75, 1684–1690.

(40) Benbouzidrollet, N. D.; Conte, M.; Guezennec, J.; Prieur, D., *J*. *Appl*. *Bacteriol*., **1991**, 71, 244–251.

(41) Lovely, D. R.; Phillips, E. J., *Appl*. *Environ*. *Microbiol*.,**1994**, 60, 726–728.

(42) Hadas, O.; Pinkas, R., *Israel*. *Microb*. *Ecol*., **1995**, 30, 55–66.

(43) Noguera, D. R.; Brusseau, G. A.; Rittmann, B. E.; Stahl, D. A., *Biotechnol*. *Bioeng*., **1998**, 59,

732–746.

(44) Tabak, H. H.; Govind, R., *Biodegradation*, **2003**, 14, 437–452.

(45) Ye, Q.; Roh, Y.; Carroll, S. L.; Blair, B.; Zhou, J.; Zhang, C. L.; Fields, M. W., *Appl*. *Environ*. *Microbiol*., **2004**, 70, 5595–5602.

(46) Heidlberg, J. F.; Seshadri, R.; Haveman, S. A.; Hemme, C. L.; Paulsen, I. T.; Kolonay, J. F.; Eisen, J. A.; Ward, N.; Methe, B.; Brinkac, L. M.; Daugherty, S. C.; Deboy, R. T.; Dodson, R. J.; Durkin, A. S.; Madupu, R.; Nelson, W. C.; Sullivan, S. A.; Fouts, D.; Haft, D. H.; Selengut, J.; Peterson, J. D.; Davidsen, T. M.; Zafar, N.; Zhou, L.; Radune, D.; Dimitrov, G.; Hance, M.; Tran, K.; Khouri, H; Gill, J.; Utterback, T. R.; Feldblyum, T. V., Wall, J. D.; Voordouw, G., Fraser, C. M., *Nat*. *Biotechnol*., **2004**, 22, 554–559.

(47) Goulhen, F.; Gloter, A.; Guyot, F.; Bruschi, M., *Appl*. *Microbiol*. *Biotechnol*., **2006**, 71, 892–897.

(48) Comisarow, M.B.; Marshall, A.G., *J*. *Chem*. *Phys*., **1976**, 64, 110–119.

(49) Marshall, A.G., *Acc*. *Chem*. *Res*., **1985**, 18, 316–322.

(50) Jokl, V.; Polášek, M.; Pospíchalová, J., *J*. *Chrom*., **1987**, 391, 427–432.

(51) Stegehuis, D.S.; Tjaden, U.R.; van der Greef, J., *J*. *Chrom*., **1992**, 591, 341–349.

(52) Baker, D. R., *Capillary Electrophoresis*. Wiley: New York; **1995**.

(53) Toussaint, B.; Hubert, Ph.; Tjaden, U.R.; van der Greef, J.; Crommen, J., *J*. *Chrom*. *A*., **2000**, 871, 173–80.

(54) Boček, P.; Gebauer P.; Deml M., *J*. *Chrom*., **1981**, 219, 21–28.

(55) Křivánková, L.; Pantůčková, P.; Boček, P., *J*. *Chrom*. *A*., **1999**, 838, 55–70.

(56) Leinweber, F. C.; Otto, M., *J*. *Chrom*. *A*, **1999**, 848, 347–363.

(57) Landers, J. P.; Handbook of Capillary Electrophoresis. CRC Press; **1997**.

FIGURE CAPTIONS

Figure 1. A schematic illustration of the normal sample stacking procedure for cationic analytes. A) The sample is introduced, under pressure, to a fused silica capillary that has been filled with the run electrolyte. B) Upon the application of a voltage, a higher electric field strength is generated within the sample plug than in the run buffer. Since electrophoretic velocity is proportional to electric field strength, the solute ions migrate rapidly through the dilute sample plug until they reach the concentration boundary between the sample plug and the run buffer, where they form narrow, stacked zones. C) Electrophoretic separation then proceeds.

Figure 2. A schematic illustration of the PMS procedure for cationic analytes. A) The NH_4OH plug, the sample, and 4 M formic acid plug are sequentially introduced, under pressure, to a fused silica capillary that has been filled with the run electrolyte. B) Upon the application of a voltage, H^+ from the 4 M formic acid plug enters the sample zone and, together with H^+ already present in the sample zone, are titrated against OH^- ions from the NH_4OH plug. C) At the point of neutrality, solute ions are stacked into narrow bands at the boundary of the titrated region and the background electrolyte. D) Electrophoretic separation then proceeds.

Figure 3. A schematic illustration of the tITP procedure for cationic analytes. A) The leading electrolyte (NH_4^+), the sample, and the terminating electrolyte (H^+), are sequentially introduced, under pressure, to a fused silica capillary that has been filled with the run electrolyte. B) Upon the application of a voltage, solute ions begin to arrange themselves in order of mobility. C) At the point of focusing, the fastest solute ions are next to the leading electrolyte, and the slowest ions are next to the terminating electrolyte. All ions then proceed to migrate at the same velocity, the velocity of the leading cations, for a transient period of time. D) Electrophoretic separation then proceeds.

Figure 4. Extracted ion mass electropherograms of 50 µM methionine sulfone via normal sample stacking and PMS-tITP. 1) Normal sample stacking with a sample injection volume of 134 nL (peak area = 21.40×10^6 counts), 2) normal sample stacking with a sample injection volume of 2.5 nL, and 3) PMS-tITP with a sample injection volume of 134 nL (peak area = 20.43×10^6 counts). Method comparison was performed using CE-FT-ICR MS.

Figure 5. Extracted ion mass electropherograms of cationic metabolites from *D. vulgaris* lysate via PMS-tITP CE-FT-ICR MS. Metabolites were identified as follows: 1) methionine sulfone (IS), 2) cytidine, 3) serine, 4) cytosine, 5) proline, 6) valine, 7) threonine, 8) 2-phenylethylamine, 9) nicotinamide, 10) nicotinic acid, 11) isoleucine, 12) leucine, 13) aspartate, 14) adenine, 15) hypoxanthine, 16) 4-aminobenzoic acid, 17) spermidine, 18) glutamine, 19) lysine, 20) glutamate, 21) methionine, 22) guanine, 23) histidine, 24) phenylalanine, 25) pyridoxine, 26) arginine, 27) tyrosine, and 28) spermine.

FIGURES

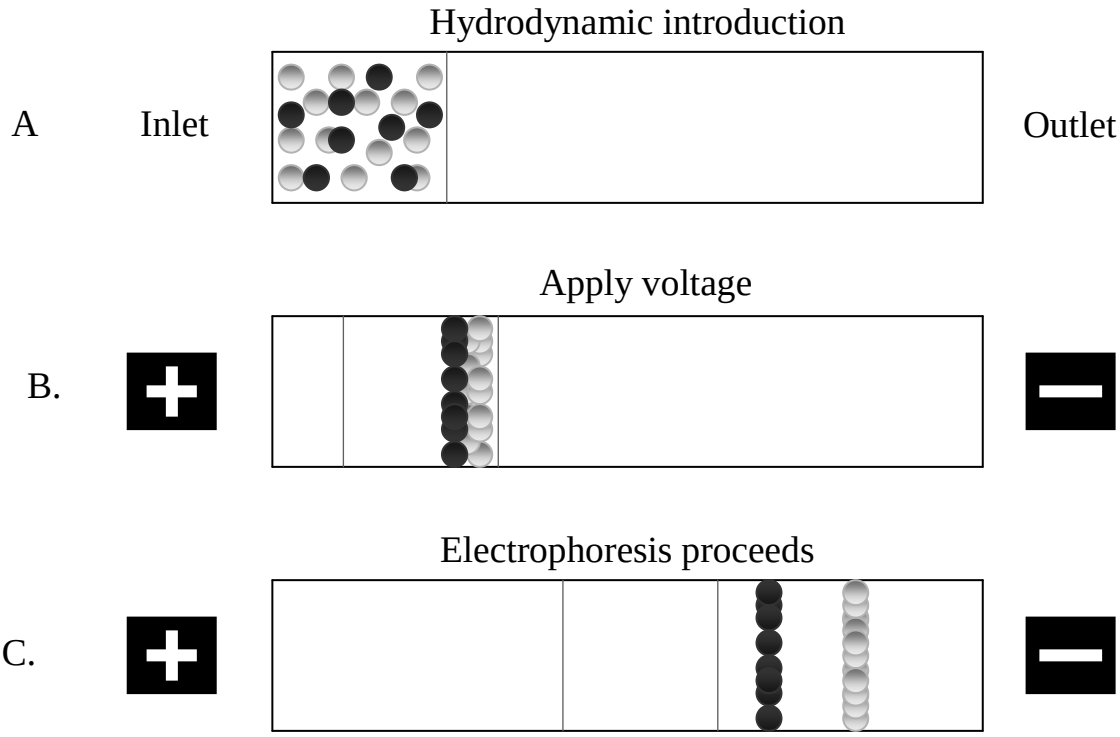

Figure 1.

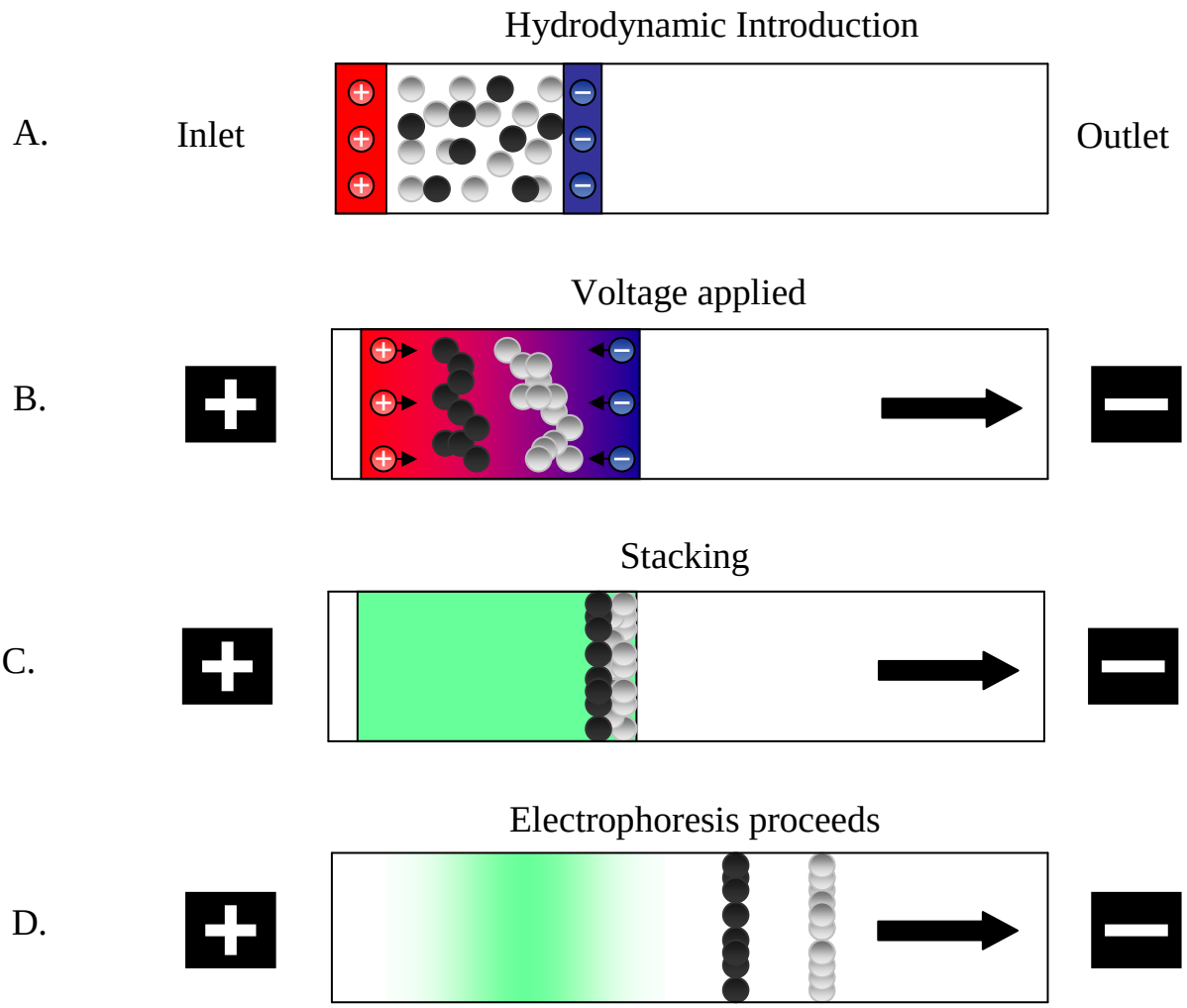
Hydrodynamic Introduction
A.
Inlet
Outlet
Voltage applied
B.
Stacking
C.
Electrophoresis proceeds
D.

Figure 2.

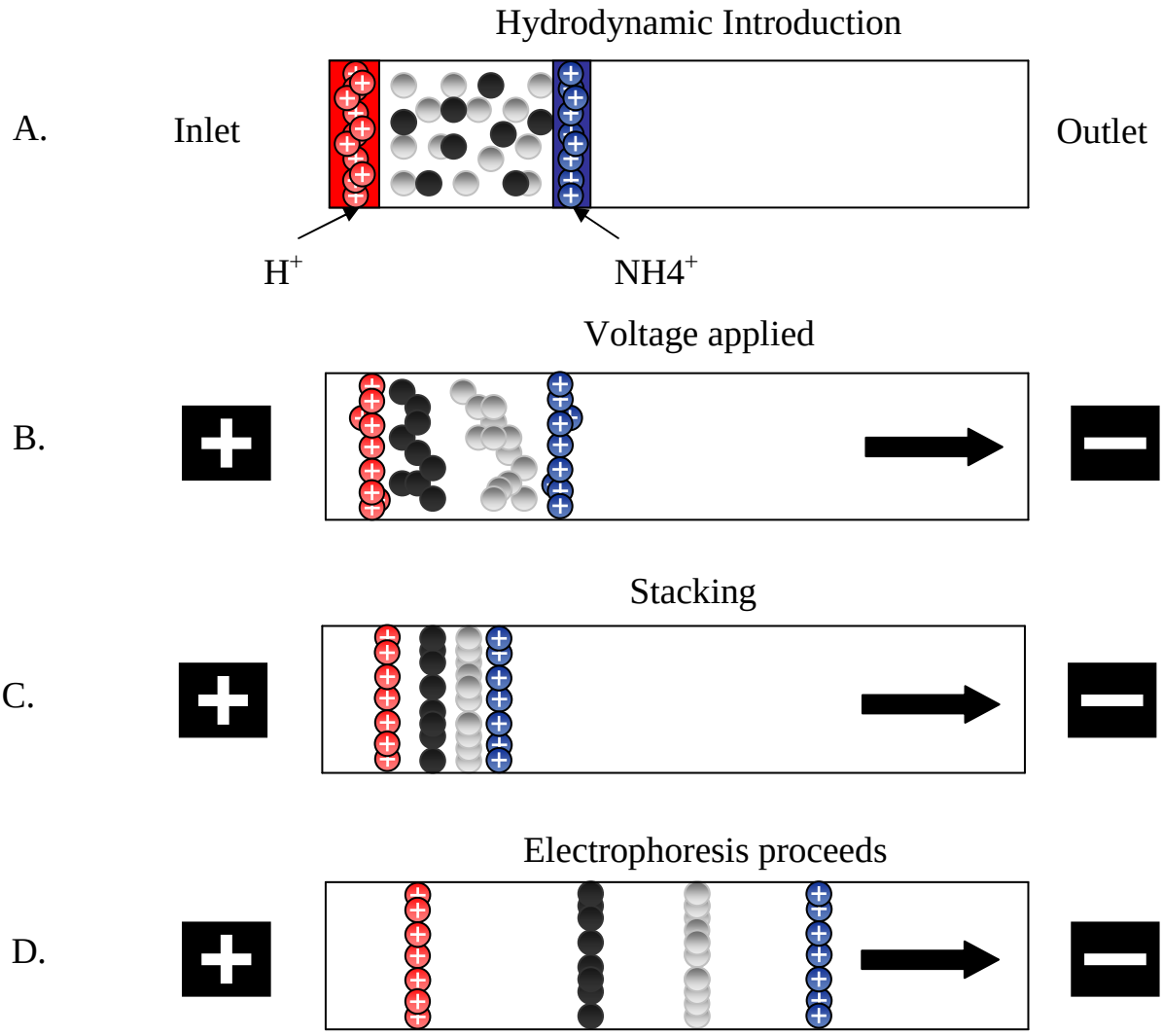
Hydrodynamic Introduction
A.
Inlet
Outlet
H+
NH4+
Voltage applied
B.
Stacking
C.
Electrophoresis proceeds
D.

Figure 3.

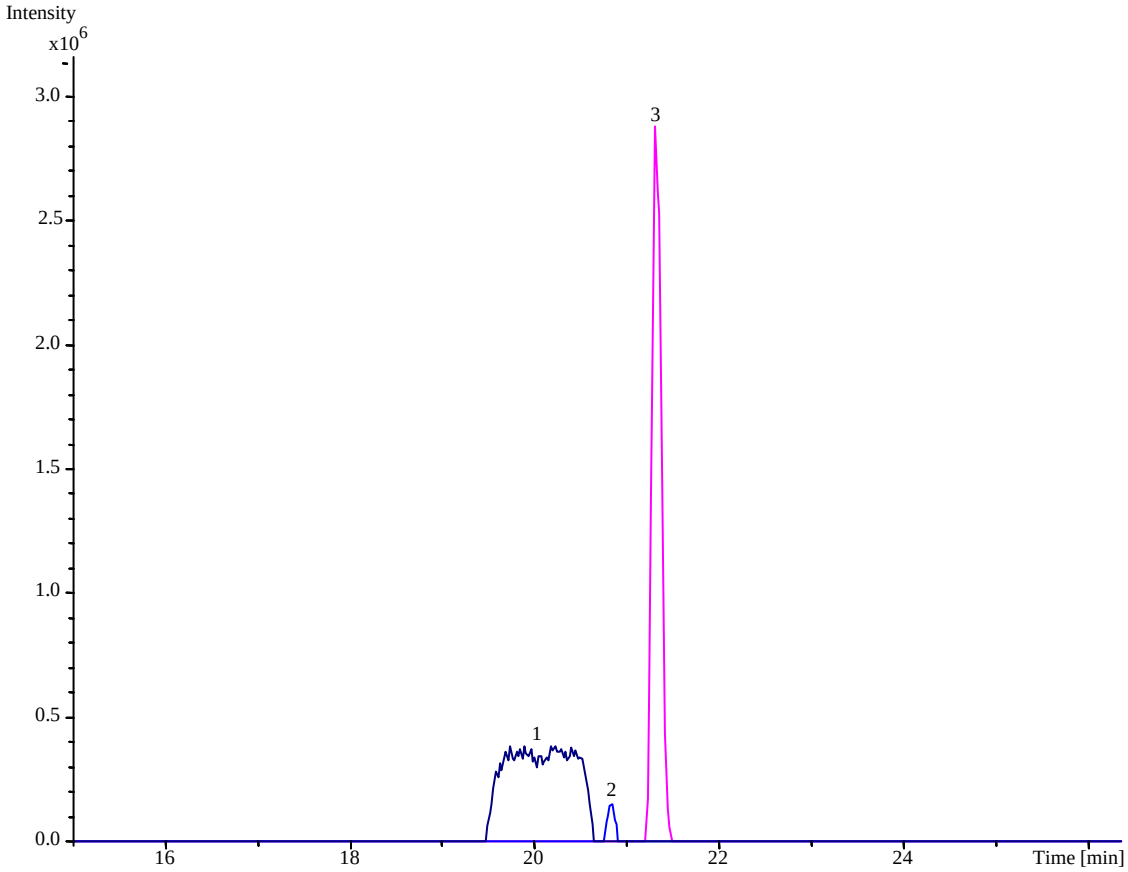

Figure 4.

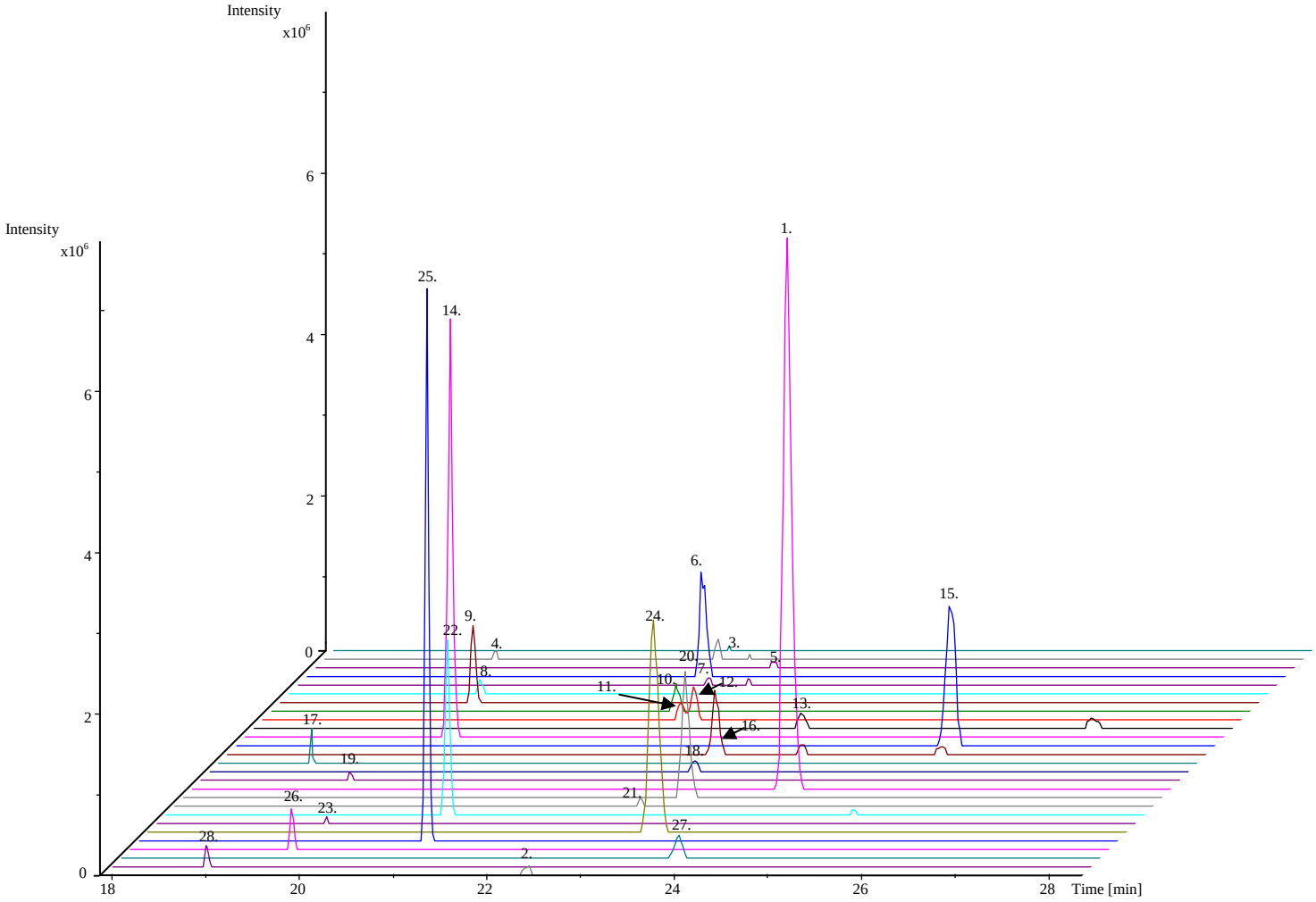
Intensity
x10^6
6
4
2
0
Intensity
x10^6
6
4
2
0
1.
25.
14.
6.
15.
9.
22.
4.
24.
3.
20.
5.
8.
7.
12.
11.
10.
13.
16.
17.
18.
19.
21.
26.
23.
27.
28.
2.
18
20
22
24
26
28
Time [min]

Figure 5.

TABLES

Table 1. Fold increases in peak area and peak height (n = 5).

	Fold increase in peak area			Fold increase in peak height		
Compound Name	NSS	PMS	Fold increase (PMS/NSS)	NSS	PMS	Fold increase (PMS/NSS)
Proline	1,374,222	58,861,029	43	256,451	11,917,151	46
Valine	1,424,441	43,334,224	30	244,256	7,307,653	30
Threonine	247,707	14,638,591	59	69,628	2,571,637	37
Isoleucine	3,047,096	52,045,800	17	554,929	8,979,150	16
Leucine	3,120,440	64,545,657	21	524,727	9,494,102	18
Glutamate	443,929	9,883,011	22	88,558	1,449,980	16
Methionine	144,849	43,473,002	300	69,985	5,909,763	84
Histidine	1,316,254	31,060,078	24	297,038	5,471,291	18
Phenylalanine	4,554,456	97,462,764	21	697,301	9,504,501	14
Arginine	2,045,387	44,502,358	22	575,516	7,310,356	13
Tyrosine	1,595,301	32,119,059	20	230,344	3,571,380	16
Met. Sulf. (IS)	853,182	20,464,369	24	149,931	2,740,972	18

Where n is the number of runs. The amino acids in the mixture used for normal sample stacking experiments were at a concentration of 50 µM. Met. Sulf. and IS are abbreviations for methionine sulfone and denotes internal standard respectively. NSS is an abbreviation for normal sample stacking.

Table 2. Resolution of selected amino acids with respect to methionine sulfone (n = 5).

Compound Name	Normal sample stacking SI at 2.5 nL	Normal sample stacking SI at 134 nL	PMS-tITP DvH sample	PMS-tITP Amino acid mixture at 3.12 µM	PMS-tITP Amino acid mixture at 50 µM
Proline	12.71	1.49	7.35	6.77	5.74
Valine	18.29	2.53	8.51	9.38	8.25
Threonine	18.22	1.77	9.93	7.90	6.49
Isoleucine	15.13	-	8.52	8.22	8.01
Leucine	13.95	-	7.56	7.65	7.26
Glutamate	10.20	0.71	3.74	4.22	3.81
Methionine	14.79	1.33	6.93	6.48	4.93
Histidine	50.35	7.18	25.54	24.50	20.96
Phenylalanine	7.00	0.65	3.20	3.55	3.21
Arginine	48.27	7.45	22.06	24.11	19.98
Tyrosine	3.26	0.44	1.57	1.47	1.48

Where n is the number of runs. The amino acids in the mixture used for normal sample stacking experiments were at a concentration of 50 µM. SI and DvH are abbreviations for sample injection and *Desulfovibrio vulgaris* Hildenborough, respectively. Peak-to-peak resolution was obtained by $R = 2(t_2-t_1)/(w_1+w_2)$. There was no separation between isoleucine and leucine for normal sample stacking with a sample injection volume of 134 nL.

Table 3. Theoretical plate numbers for selected amino acids (n = 5).

Compound Name	Normal sample stacking SI at 2.5 nL	Normal sample stacking SI at 134 nL	PMS-tITP DvH sample	PMS-tITP Amino acid mixture at 3.12 µM	PMS-tITP Amino acid mixture at 50 µM
Proline	177,402	4,502	1,050,510	199,544	87,270
Valine	166,445	6,414	203,769	191,498	69,689
Threonine	718,950	9,961	1,027,274	518,556	126,646
Isoleucine	135,082	-	453,243	190,329	122,844
Leucine	132,337	-	342,088	199,895	102,707
Glutamate	484,714	6,407	174,192	291,911	78,284
Methionine	472,444	6,019	1,082,640	363,807	66,410
Histidine	178,760	7,363	2,822,400	238,408	83,571
Phenylalanine	127,400	4,535	106,285	119,629	45,905
Arginine	120,136	7,235	501,366	171,706	55,760
Tyrosine	167,670	5,298	227,739	184,553	56,099

Where n is the number of runs. The amino acids in the mixture used for normal sample stacking experiments were at a concentration of 50 µM. SI and DvH are abbreviations for sample injection and *Desulfovibrio vulgaris* Hildenborough respectively. Theoretical plate numbers were obtained by $N = 16(t/w)^2$. There was no separation between isoleucine and leucine for normal sample stacking with a sample injection volume of 134 nL.

Table 4. Linearity and limits of detection and quantitation of selected amino acids.

Compound Name	R^2	LOD (µM, s/n = 3)	LOQ (µM, s/n = 10)
Alanine[1]	0.9972	0.57	1.91
Serine[1]	0.9944	0.28	0.94
Proline[2]	0.9949	0.14	0.46
Valine[2]	0.9932	0.18	0.61
Threonine[1]	0.9928	0.55	1.85
Isoleucine[2]	0.9971	0.38	1.28
Leucine[2]	0.9989	0.37	1.25
Aspartate[1]	0.9948	0.64	2.13
Lysine[3]	0.9995	0.47	1.56
Methionine[3]	0.9903	1.99	6.65
Histidine[4]	0.9996	0.44	1.48
Phenylalanine[4]	0.9980	0.10	0.34
Arginine[2]	1.0000	0.34	1.14
Tyrosine[4]	0.9987	1.59	5.30

Where s/n, LOD and LOQ are the signal-to-noise, limit of detection and limit of quantitation respectively. The number 1 denotes a five-point calibration curve over a dynamic range of 3.12 to 50 µM. The number 2 denotes a six-point calibration curve over a dynamic range of 0.78 to 25 µM. The number 3 denotes a six-point calibration curve over a dynamic range of 1.56 to 50 µM. The number 4 denotes a seven-point calibration curve over a dynamic range of 0.78 to 50 µM.

Table 5. Metabolites identified from *D. vulgaris* lysate (n = 5).

Compound Name	Calculated m/z	Measured m/z	Mass Error (ppm)	RMT	Concentration pM
Methionine Sulfone (IS)	182.048155	182.048061	0.52	1.000	
Serine	106.049870	106.049741	1.22	0.913	92
Cytosine	112.050538	112.050564	-0.23	0.815	
Proline	116.070605	116.070691	-0.74	0.940	136
Valine	118.086255	118.086268	-0.11	0.912	771
Threonine	120.065520	120.065472	-0.40	0.919	271
2-Phenylethylamine	122.096426	122.096410	0.13	0.823	
Nicotinamide	123.055289	123.055279	0.08	0.824	
Nicotinic acid	124.039305	124.039282	0.19	0.916	
Isoleucine	132.101905	132.101889	0.12	0.923	154
Leucine	132.101905	132.101935	-0.23	0.928	176
Aspartate	134.044784	134.044854	-0.52	0.979	838
Adenine	136.061772	136.061705	0.49	0.829	
Hypoxanthine	137.045787	137.045823	-0.26	1.052	
4-Aminobenzoic acid	138.054955	138.054928	0.20	0.953	
Spermidine	146.165174	146.165114	0.41	0.780	
Glutamine	147.076419	147.076872	-3.08	0.952	
Lysine	147.112804	147.112959	-1.05	0.804	61
Glutamate	148.060434	148.060445	-0.07	0.959	
Methionine	150.058326	150.058260	0.44	0.944	174
Guanine	152.056686	152.056722	-0.24	0.863	
Histidine	156.076753	156.077049	-1.90	0.814	50
Phenylalanine	166.086255	166.086242	0.08	0.961	21
Pyridoxine	170.081170	170.080677	2.90	0.865	
Arginine	175.118952	175.118841	0.63	0.810	220
Tyrosine	182.081170	182.081249	-0.43	0.984	45
Spermine	203.223023	203.222777	1.21	0.780	
Cytidine	244.092797	244.092381	1.70	0.925	

Where n is the number of runs and IS is the internal standard. RMT is the relative migration time (i.e. the migration time of the metabolite divided by the migration time of the internal standard). Concentrations were calculated via calibration curves (Supporting Information Figure 2) and percent recoveries on the Oasis HLB SPE cartridge (data not shown), and are in pM per mL of cell culture.